





Exactly solvable model of a slightly fluctuating ratchetV. M. Rozenbaum ^{1,*}, T. Ye. Korochkova ¹, I. V. Shapochkina ² and L. I. Trakhtenberg ³¹*Chuiiko Institute of Surface Chemistry, National Academy of Sciences of Ukraine, Generala Naumova str. 17, Kiev 03164, Ukraine*²*Department of Physics, Belarusian State University, Prospekt Nezavisimosti 4, Minsk 220050, Belarus*³*Semenov Federal Research Center of Chemical Physics, Russian Academy of Sciences, Kosygin Street 4, Moscow 119991, Russia; Moscow Institute of Physics and Technology, Institutsky Lane 9, Dolgoprudny 141700, Moscow Region, Russia; and Lomonosov Moscow State University, 1–3 Leninskie gory, Moscow, 119991, Russia*

(Received 23 March 2021; revised 1 June 2021; accepted 24 June 2021; published 26 July 2021)

We consider the motion of a Brownian particle in a sawtooth potential dichotomously modulated by a spatially harmonic perturbation. An explicit expression for the Laplace transform of the Green function of an extremely asymmetric sawtooth potential is obtained. With this result, within the approximation of small potential-energy fluctuations, the integration of the relations for the average particle velocity is performed in elementary terms. The obtained analytical result, its high-temperature, low-frequency, and high-frequency asymptotics, as well as numerical calculations performed for a sawtooth potential of an arbitrary symmetry, indicate that in such a system, the frequency-temperature controlling the magnitude and direction of the ratchet velocity becomes possible. We clarify the mechanism of the appearance of additional regions of nonmonotonicity in the frequency dependence of the average velocity, which leads to the appearance of additional ratchet stopping points. This mechanism is a consequence of the competition between the sliding time along the steep slope of the highly asymmetric sawtooth potential and the correlation time of the dichotomous noise.

DOI: [10.1103/PhysRevE.104.014133](https://doi.org/10.1103/PhysRevE.104.014133)**I. INTRODUCTION**

One of the mechanisms through which nanoparticle transport can be realized is the use of the ratchet effect, the phenomenon of appearance of directed motion in a nanosystem, being in contact with a thermostat, due to unbiased nonequilibrium perturbations of various nature under the broken spatial and (or) temporal symmetry [1–5]. The advantage of such a mechanism is in the effectiveness of controlling the motion characteristics that the ratchet effect can provide. One can control the transport through variations of a number of parameters, individually or their combinations: particle size, temperature, medium viscosity, fluctuation frequency of the nanoparticle potential energy, the form of the dependence of fluctuations on time and coordinate and, finally, the spatial shape of a stationary part of a potential relief in which the particles move. The theoretical linking the change in parameters of a ratchet system to the direction and magnitude of the induced motion can be important in solving a number of applied problems, such as studying functioning of protein motors in a living cell [6], design of molecular machines capable of manipulating membrane components, proteins, and lipids [7], which is very important for functional research [8,9]. It is also important in design (synthesis) of various artificial molecular analogs of protein motors [10–12]: DNA walkers, which can jump along substrates and function as programmable assembly lines [13–18], nanomachines capable of dragging nanoloads [19], and other synthetic molecular motors, trans-

lational and rotational [20–22]. Modern computational tools make it possible to calculate the motion characteristics in almost any chosen specific conditions, to simulate experimental results, which require a great deal of efforts to be obtained [23]. However, such calculations are not of high heuristic value, since too many numerical experimentations are required to gain knowledge about the factors affecting, in one way or another, the motion control.

Under these conditions, analytical solutions of complex equations of motion acquire special value. These solutions are explicit functions of parameters characterizing the factors listed above. They allow us to judge which changes in the control factors can lead to certain (desired) changes in motion characteristics. Naturally, to obtain analytical solutions, one should use approximations as well as operate with simplified shapes of potential reliefs and control signals. At present, the most fruitful approximations are (i) the approximations of small or large potential barriers, relative to the thermal energy, i.e., the so-called high-temperature approximation or kinetic approach, respectively; (ii) low-frequency (adiabatic) or high-frequency approximations, in which the disturbance frequency (inverse correlation time) is small or large in comparison with the characteristic frequencies of the system, respectively; and (iii) the piecewise linear shape of a potential relief [24]. The disadvantages of all these approximations are in the limitations of the results that follow from them with respect to the set of control parameters. For example, the high-temperature results cannot predict the way in which one could control the motion characteristics by tuning the temperature, while the low-frequency and high-frequency results cannot predict the way to do that by tuning the frequency.

*Corresponding author: vik-roz@mail.ru

The approximation of slightly fluctuating potential energy is able to get over the listed difficulties in developing analytical approaches to the problems of nanotransport control [25]. Within this approximation, not the entire potential profile as a whole, but its fluctuations relative to the thermal energy are considered small. Main relations of the theory of slightly fluctuating ratchets are given in the introductory Sec. II (the detailed derivation is in Appendix A). They are of great generality, but, at the same time, they are written through a complex double integral containing the Green function, which describes diffusion in a given periodic potential relief. An explicit analytical expression can only be obtained for the Laplace transform of the Green function of a piecewise linear potential relief; and this transform is too cumbersome so that the analytical calculation of the integral is hardly possible [24]. In this paper, we consider an extremely asymmetric sawtooth potential modulated by a weak spatially harmonic perturbation, the time dependence of which is described by a stochastic dichotomous process. With these simplifications, it became possible not only to obtain a simple form of the Green function (Sec. III), but also to take the double integral analytically. As a result, a rather compact analytical expression for the average velocity of directed motion has been obtained (Sec. IV); its asymptotics are given in Sec. V. The temperature and fluctuation-frequency dependences of the obtained expressions turned out to be nontrivial. The same dependences obtained numerically for a sawtooth potential of arbitrary symmetry (Sec. VI) turned out to be even more nontrivial. The analysis of the results explains how additional stopping points can originate from the competition of the system characteristic times (namely the sliding time along the steep slope of the highly asymmetric sawtooth potential and the correlation time of the dichotomous noise), when the symmetry parameter of the sawtooth potential is reaching of its limit value; it also demonstrates the ways to control the motion direction by changing the temperature and perturbation frequency values (Sec. VII). Symmetry analysis (given in Appendix B) allowed us to narrow the definition domains of the parameters used.

II. SLIGHTLY FLUCTUATING RATCHET

Consider the overdamped motion of a Brownian particle characterized by the potential energy, the space-time dependence of which has the following additive-multiplicative form:

$$U(x, t) = u(x) + \sigma(t)w(x). \quad (1)$$

The stationary potential relief, $u(x)$, and the multiplicative term, $\sigma(t)w(x)$, are a main contribution and a small correction, respectively. Expression (1) covers the majority of significant, practically and theoretically, cases of potential-energy changes [1,2,26]. Assuming that the functions $u(x)$ and $w'(x) \equiv dw(x)/dx$ are L periodic, one can treat flashing and rocking ratchets, which are the two main models in the theory of Brownian motors, in a similar fashion by means of relation (1). In this paper, we will deal only with flashing ratchets; the function $w(x)$ itself can thus also be considered L periodic. The function $\sigma(t)$ describes the features of temporal fluctuations of the particle potential energy. As $\sigma(t)$ plays

the role of a fluctuation variable, it must have the zero mean value, $\langle \sigma(t) \rangle = 0$; the symbol $\langle \dots \rangle$ means the operation of averaging over fluctuations, the definition of which depends on the nature of the quantity $\sigma(t)$.

The main quantity of interest in the theory of ratchet systems, including the slightly fluctuating ratchets, is the average particle velocity, $\langle v \rangle$, called the ratchet velocity. Having applied the perturbation theory for the Smoluchowski equation with respect to a small value $w'(x)$, one can write this velocity in the following form [25] (see the detailed derivation in Appendix A):

$$\langle v \rangle = L\beta^2 D^2 \int_0^L dx \rho_+(x) w'(x) \int_0^L dy S(x, y) \frac{\partial}{\partial y} [w'(y) \rho_-(y)],$$

$$\rho_{\pm}(x) = e^{\pm\beta u(x)} \int_0^L dx e^{\pm\beta u(x)}, \quad (2)$$

where $D = (\beta\zeta)^{-1}$ is the diffusion coefficient, ζ is the friction coefficient, $\beta = (k_B T)^{-1}$ is the inverse thermal energy (k_B is the Boltzmann constant, T is the absolute temperature), and $\rho_{\pm}(x)$ is the equilibrium Boltzmann distribution in the stationary potential profile $u(x)$. The function $S(x, y)$ is determined by the following relation:

$$S(x, y) = \int_0^{\infty} dt g(x, y, t) K(t), \quad (3)$$

where $K(t) \equiv \langle \sigma(t_0 + t)\sigma(t_0) \rangle$ is the correlation function of the second order, and $g(x, y, t)$ is the retarded Green function [$g(x, y, t) = 0$ at $t < 0$] of diffusion in the stationary potential relief $u(x)$, satisfying the equation

$$\frac{\partial}{\partial t} g(x, y, t - t') + \frac{\partial}{\partial x} [\hat{J}(x)g(x, y, t - t')] = -\delta(x - y)\delta(t - t') \quad (4)$$

with the flux operator

$$\hat{J}(x) = -De^{-\beta u(x)}(\partial/\partial x)e^{\beta u(x)}. \quad (5)$$

The character of the dependence of the average velocity on parameters of the ratchet system is determined by the features of the function $S(x, y)$ which describes the process of particle propagation from a point y to a point x in the potential $u(x)$. In this paper, we will deal with the particle motion under the perturbations induced by a stochastic dichotomous process with an inverse correlation time Γ ; the correlation function is thus determined as $K(t) = \exp(-\Gamma|t|)$. For such a process, according to relation (3), the function $S(x, y)$ is interpreted as the Laplace image of the Green function $g(x, y, t)$. Therefore, in what follows, for brevity, we will also use the name ‘‘the Green function’’ for the function $S(x, y)$ itself. Termwise multiplying Eq. (4) by $\exp(-\Gamma t)$, integrating the result over t from $-\varepsilon$ to ∞ (where ε is an infinitely small positive quantity), and taking into account that the term $\exp(\Gamma\varepsilon)g(x, y, -\varepsilon)$ is zero [because of the fact that $g(x, y, t)$ is the retarded Green

function], yields the following equation:

$$\left[\frac{d}{dx} \hat{J}(x) + \Gamma \right] S(x, y) = -\delta(x - y). \quad (6)$$

For the stochastic dichotomous process, the physical meaning of the function $S(x, y)$ is stated as following: The quantity $-\Gamma S(x, y)$ specifies the probability density of finding a particle at a point x in the state characterized by the lifetime Γ^{-1} and the potential $u(x)$, provided that the particle was originally placed at a point y . In the high-frequency limit, $\Gamma \rightarrow \infty$, and if the potential relief $u(x)$ is described by a smooth function, Eq. (6) yields the approximate equality $-\Gamma S(x, y) = \delta(x - y)$, substitution of which into Eq. (2) gives the following expression for the average velocity [1,24,27,28]:

$$\langle v \rangle = \frac{LD^2\beta^3}{\Gamma} \frac{\int_0^L dx u'(x) [w'(x)]^2}{\int_0^L dx e^{\beta u(x)} \int_0^L dx e^{-\beta u(x)}}. \quad (7)$$

In the next section, we calculate the function $S(x, y)$ for the extremely asymmetric stationary potential relief $u(x)$; the result will allow us to develop an analytical expression for the average velocity defined by the relation (2).

III. GREEN FUNCTION FOR THE CASE OF AN EXTREMELY ASYMMETRIC SAWTOOTH POTENTIAL

Assume that the Green function $S(x, y)$ satisfying Eq. (6) is L periodic in both variables, x and y , and has no discontinuities of the second kind. Let us introduce the function $\tilde{J}(x, y) = -\hat{J}(x)S(x, y)$ with the following physical meaning: The quantity $\Gamma \tilde{J}(x, y)$ specifies the particle flux in the state with the lifetime Γ^{-1} through a cross section x in the potential $u(x)$, provided that originally the particles were placed at a point y . For brevity, we will call the function $\tilde{J}(x, y)$ the flux. Termwise integration of Eq. (6) over x from $x_0 - \kappa$ to $x_0 + \kappa$ with positive κ values which tend to zero leads to the condition

$$\tilde{J}(x_0 + \kappa, y) - \tilde{J}(x_0 - \kappa, y) \xrightarrow{\kappa \rightarrow 0} \begin{cases} 1, & x_0 = y, \\ 0, & x_0 \neq y, \end{cases} \quad (8)$$

which means that the flux $\tilde{J}(x, y)$ is continuous for all $x \neq y$ and has the unit jump at $x = y$.

Among different shapes of potential profiles, piecewise-linear profiles are those for which an analytical solution of the differential equation (6) is most easily obtained, and a special place here belongs to a sawtooth potential, with the widths of its links l and $L - l$ [24]. Such a potential is a most convenient choice to introduce an asymmetry into a ratchet model, since the asymmetry of the sawtooth potential is easily controlled by changing only the parameter l . The limiting cases $l \rightarrow 0$, L allow studying the singularity properties of system characteristics introduced by jumps emerging in the potential profile [25,29–31]. Moreover, a sawtooth shape can be easily realized experimentally [32]. In numerous experiments on directed motion of colloidal particles, sawtooth shapes of the ratchet potential are created by means of interdigitated electrodes, deposited on the glass slides using photolithographic techniques (see, e.g., Chap. 7 in Ref. [4]). In experiments for manipulating charged components within supported lipid bilayers [33], such ratchet potential is created by a patterned bilayer (its one side is of a sawtooth shape while its opposite side is a planar

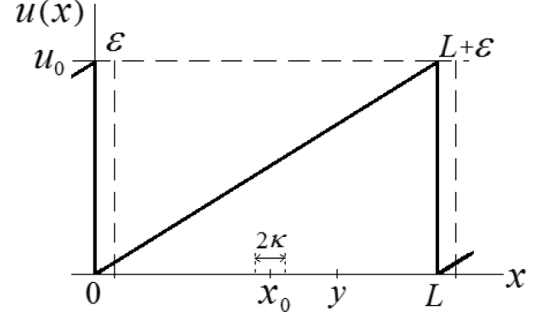


FIG. 1. Extremely asymmetric sawtooth potential profile $u(x)$, having a jump u_0 at a point $l = L$, plotted in the interval $(\epsilon, L + \epsilon)$.

surface). An external electric field either drives the charged lipids into a region of free diffusion or concentrates them in the teeth.

We will define the extremely asymmetric ($l = L$) sawtooth potential $u(x)$ on the interval $(\epsilon, L + \epsilon)$ in such a way that the jump u_0 appears at the point $x = L$ (Fig. 1),

$$u(x) = u_0(x/L - \theta(x - L)), \quad x \in (\epsilon, L + \epsilon), \quad 0 < \epsilon \rightarrow 0 \quad (9)$$

[$\theta(x)$ is the theta function equal to 1 for $x > 0$ and 0 for $x < 0$]. Using the definition (5) of the flux operator, we multiply (term by term) the equation $\tilde{J}(x, y) = -\hat{J}(x)S(x, y)$ by $\exp[\beta u(x)]$ and integrate the result over x from $L - \epsilon$ to $L + \epsilon$:

$$\begin{aligned} & e^{\beta u(L + \epsilon)} S(L + \epsilon, y) - e^{\beta u(L - \epsilon)} S(L - \epsilon, y) \\ &= D^{-1} \int_{L - \epsilon}^{L + \epsilon} dx e^{\beta u(x)} \tilde{J}(x, y). \end{aligned} \quad (10)$$

The integral on the right-hand side of Eq. (10) tends to zero at $\epsilon \rightarrow 0$ not only when $y \neq L$, with the flux $J(x, y)$ continuous in the vicinity of the point $x = L$, but also at $y = L$, when there exists a jump described by the relation (8) with $x_0 = L$. Taking into account the designations

$$u(L - \epsilon) \xrightarrow{\epsilon \rightarrow 0} u_0, \quad S(L - \epsilon, y) \xrightarrow{\epsilon \rightarrow 0} S(L - 0, y) \quad (11)$$

and the periodicity conditions

$$u(L + \epsilon) = u(\epsilon) \xrightarrow{\epsilon \rightarrow 0} 0, \quad S(L + \epsilon, y) \xrightarrow{\epsilon \rightarrow 0} S(+0, y), \quad (12)$$

we derive the following boundary condition:

$$S(+0, y) = e^\alpha S(L - 0, y), \quad \alpha \equiv \beta u_0. \quad (13)$$

With the extremely asymmetric sawtooth potential (9) corresponding to the state with the lifetime Γ^{-1} , the original Eq. (6) becomes a constant-coefficient second-order differential equation:

$$L^2 \frac{\partial^2}{\partial x^2} S(x, y) + \alpha L \frac{\partial}{\partial x} S(x, y) + \lambda^2 S(x, y) = 0, \quad \lambda^2 = \frac{\Gamma L^2}{D}, \quad (14)$$

provided that $x \neq y$, L . Its general solutions in the intervals $x \in (+0, y)$ and $x \in (y, L-0)$,

$$\begin{aligned} S^l(x, y) &= A_1^l e^{\Lambda_1 x/L} + A_2^l e^{\Lambda_2 x/L}, \\ S^r(x, y) &= A_1^r e^{\Lambda_1 x/L} + A_2^r e^{\Lambda_2 x/L} \end{aligned} \quad (15)$$

with parameters

$$\Lambda_{1,2} = -\frac{\alpha}{2} \pm \sqrt{\frac{\alpha^2}{4} + \lambda^2}, \quad (16)$$

$$\begin{aligned} S^{l,r}(x, y) &= \frac{L}{D(\Lambda_1 - \Lambda_2)\text{Det}(\hat{1} - \hat{C})} \sum_{k,m=1,2} (-1)^{m-1} a_{km}^{l,r} e^{\Lambda_k x/L - \Lambda_m y/L}, \\ \hat{a}^l &= \hat{C} - \hat{1}, \quad \hat{C} = \frac{1}{\Lambda_1 - \Lambda_2} \begin{pmatrix} \Lambda_1 e^{-\Lambda_2} - \Lambda_2 e^{\Lambda_1} & \Lambda_1 (e^{-\Lambda_1} - e^{\Lambda_2}) \\ \Lambda_2 (e^{\Lambda_1} - e^{-\Lambda_2}) & \Lambda_1 e^{\Lambda_2} - \Lambda_2 e^{-\Lambda_1} \end{pmatrix}, \\ \hat{a}^r &= \hat{1} - \hat{C}^{-1}, \quad \hat{C}^{-1} = \frac{1}{\Lambda_1 - \Lambda_2} \begin{pmatrix} \Lambda_1 e^{\Lambda_2} - \Lambda_2 e^{-\Lambda_1} & -\Lambda_1 (e^{-\Lambda_1} - e^{\Lambda_2}) \\ -\Lambda_2 (e^{\Lambda_1} - e^{-\Lambda_2}) & \Lambda_1 e^{-\Lambda_2} - \Lambda_2 e^{\Lambda_1} \end{pmatrix}, \\ \text{Det}(1 - \hat{C}) &= \frac{4}{\Lambda_1 - \Lambda_2} \left(\Lambda_2 \sinh^2 \frac{\Lambda_1}{2} - \Lambda_1 \sinh^2 \frac{\Lambda_2}{2} \right). \end{aligned} \quad (18)$$

The surface in Fig. 2 represents the function $S(x, y)$ in the basic region of values of its arguments x and y . This surface, described by a dimensionless positive quantity $-\Gamma LS(x, y)$, illustrates the probability density $-\Gamma S(x, y)$ of finding a particle at the point x if it was originally located at the point y . If the lifetime of the state with the potential $u(x)$ tends to zero ($\Gamma \rightarrow \infty$), then $-\Gamma LS(x, y) \rightarrow L\delta(x-y)$. Therefore, at finite Γ , the surface contains the line of cusp points corresponding to $x = y$. The $S(x, y)$ surface also demonstrates both the jumps at the boundaries $x = 0$ and $x = L$ of the region when changing x values and continuity at the boundaries $y = 0$ and $y = L$ when changing y values [see relations (17)]. Note that in the long-lived potentials ($\Gamma \rightarrow 0$) the dependence on the initial particle position disappears, and the function $-\Gamma S(x, y)$ tends

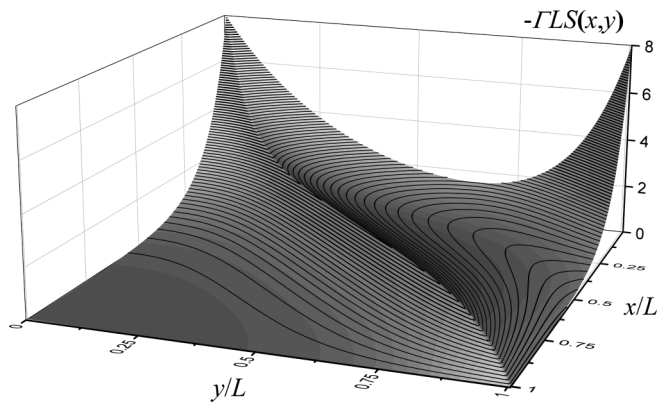


FIG. 2. Surface plot for the function $-\Gamma LS(x, y)$ at fixed values of parameters: $\alpha = \beta u_0 = 5$ (dimensionless inverse temperature) and $\lambda^2 = \Gamma L^2/D = 25$ (the dimensionless inverse correlation time). The function $-\Gamma LS(x, y)$ is the dimensionless probability density of finding a particle at the point x if it was originally located at the point y .

contain four arbitrary constants $A_1^{l,r}$, $A_2^{l,r}$ which can be determined from the four boundary conditions:

$$\begin{aligned} S(y-0, y) &= S(y+0, y), \quad \tilde{J}(y+0, y) - \tilde{J}(y-0, y) = 1, \\ S(+0, y) &= e^\alpha S(L-0, y), \quad \tilde{J}(+0, y) = \tilde{J}(L-0, y). \end{aligned} \quad (17)$$

The particular solution of Eq. (14), obtained in this way with boundary conditions (17), can be represented in the following compact form:

to the equilibrium Boltzmann distribution in the stationary potential $u(x)$ [see the expression for $\rho_-(x)$ in Eq. (2)].

IV. AVERAGE PARTICLE VELOCITY

For the extremely asymmetric sawtooth potential $u(x)$, the calculating procedure for the average particle velocity by means of Eq. (2) can be complex due to the presence of a generalized function in the derivative of the Boltzmann distribution, $\partial \rho_-(y)/\partial y$, in a stepwise potential. Therefore, it is

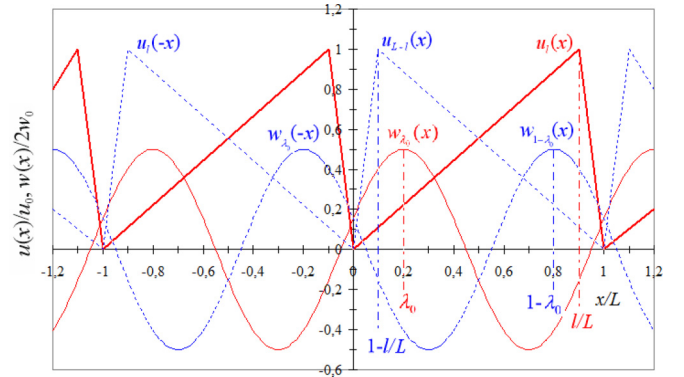


FIG. 3. Geometry of the components, stationary $u(x)$ and fluctuating $w(x)$, of the nanoparticle potential energy of the additive-multiplicative form (1), demonstrating the symmetry properties $u_l(-x) = u_{L-l}(x)$, $w_{\lambda_0}(-x) = w_{1-\lambda_0}(x)$, $w_{\lambda_0-1/2}(x) = -w_{\lambda_0}(x)$, and $w_{\lambda_0}(x+L/2) = w_{\lambda_0-1/2}(x)$ (the subscripts denote main parameters in the chosen geometry; L is the period, l and λ_0 are the coordinate of the peak of the sawtooth profile $u(x)$ and the phase shift of the cosine perturbation $w(x)$, respectively). When $l = L$, the sawtooth profile $u(x)$ becomes extremely asymmetric. The symmetry properties are used in Appendix B for constructing chains of symmetry transformations of the ratchet average velocity.

reasonable to integrate the inner integral by parts and apply the periodicity of all the integrands to rearrange the double integral to the following form:

$$\langle v \rangle = -L\beta^2 D^2 \int_{+0}^{L-0} dx \rho_+(x) w'(x) \times \int_{+0}^{L-0} dy w'(y) \rho_-(y) \frac{\partial}{\partial y} S(x, y). \quad (19)$$

Here, the derivative $\partial S(x, y)/\partial y$ has a discontinuity of the first kind (jump) at the point $y = x$, which does not complicate taking the inner integral; on the interval $(+0, L-0)$, the functions $\rho_{\pm}(x)$ are equal to

$$\rho_{\pm}(x) = \frac{e^{\pm\alpha x/L}}{L \varphi_1(\alpha)}, \quad \varphi_1(\alpha) = \frac{\sinh(\alpha/2)}{\alpha/2} \quad (20)$$

and have no special features.

$$\begin{aligned} \frac{\langle v \rangle}{v_0} &= \frac{2\pi^2 \alpha^3 \gamma}{\varphi_1^2(\alpha) f(\alpha, \gamma)} \left\{ \frac{\cosh \delta - \cosh(\alpha/2)}{\Delta(\alpha, \gamma)} \varphi_1(\alpha) \left[\cos 4\pi \lambda_0 - 1 + \frac{8\pi^2 \alpha^2}{f(\alpha, \gamma)} \right] + 1 \right\}, \\ f(\alpha, \gamma) &= (\Lambda_1^2 + (2\pi)^2)(\Lambda_2^2 + (2\pi)^2), \quad \Lambda_{1,2} = -\frac{\alpha}{2} \pm \delta, \quad \delta = \sqrt{\left(\frac{\alpha}{2}\right)^2 + \alpha\gamma}, \\ \Delta(\alpha, \gamma) &= \cosh \delta \cosh \frac{\alpha}{2} - 1 - \frac{\alpha}{2\delta} \sinh \delta \sinh \frac{\alpha}{2}. \end{aligned} \quad (22)$$

Here, the main parameters are $\alpha \equiv \beta u_0$ (dimensionless inverse temperature) and $\gamma \equiv \Gamma \tau_L$ (dimensionless fluctuation frequency). The average ratchet velocity is measured in units $v_0 = (w/u)^2 (L/\tau_L)$, where $\tau_L \equiv \zeta L^2/u_0$ is the sliding time along the gentle slope of the extremely asymmetric sawtooth potential.

Relationship (22) is the main analytical result of this paper; in the subsequent sections we will analyze it in detail and in different contexts. Here, we only note that the phase shift λ_0 enters the expression (22) by means of the function $\cos 4\pi \lambda_0$, invariant under the transformation $\lambda_0 \rightarrow 1/2 - \lambda_0$. In Appendix B, it is shown [see Eq. (B10)] that this symmetry property is inherent in general solutions of the considered model as a model describing the overdamped motion (that is, the property is not a consequence of the used approximation of slight fluctuations) and valid for arbitrary time dependences of fluctuations of the universal symmetry type.

V. ASYMPTOTIC EXPRESSIONS

Within the above model, extended additionally by the assumption about arbitrary values of the widths l and $L-l$, an asymptotic expression for the average velocity valid for high temperatures ($\alpha \rightarrow 0$) can be obtained [34]:

$$\begin{aligned} \frac{\langle v \rangle}{v_0} &\xrightarrow{\alpha \rightarrow 0} -\pi \alpha^2 \varphi_2(\lambda^2) f(l, \lambda_0), \\ \varphi_2(\lambda^2) &= \frac{\lambda^2}{(\lambda^2 + 4\pi^2)^2}, \quad \lambda^2 = \alpha\gamma \\ f(l, \lambda_0) &= \frac{L}{l(L-l)} \sin 2\pi(l/L) \cos 2\pi(l/L - 2\lambda_0). \end{aligned} \quad (23)$$

To control the ratchet motion, we choose a dichotomous process with the spatially harmonic perturbation of the form (Fig. 3)

$$w(x) = w \cos[2\pi(x/L - \lambda_0)]. \quad (21)$$

The sinusoidal-shaped perturbation $w(x)$ of an amplitude w and a phase shift λ_0 is a reasonable choice to model an external influence on the system in many cases, when the influence is of an artificial nature (introduced by man-made mechanisms) [34].

For the Green function (18) of the extremely asymmetric sawtooth potential and the coordinate dependence (21) of the slight perturbation, the integrals in Eq. (19) are reduced to integrals of the products of exponential and trigonometric functions, which can be taken analytically. Simplifying the cumbersome result of the double integration leads us to the following expression:

At $l \rightarrow L$, the function $f(l, \lambda_0)$ tends to $f(L, \lambda_0) = -2\pi \cos 4\pi \lambda_0$, and formula (23) becomes

$$\frac{\langle v \rangle}{v_0} \xrightarrow{\alpha \rightarrow 0} 2\pi^2 \alpha^2 \varphi_2(\lambda^2) \cos 4\pi \lambda_0. \quad (24)$$

The result (24) can also be obtained by the asymptotic expansion of the ‘‘extremely asymmetric’’ expression (22) with $\alpha \rightarrow 0$ (high-temperature limit).

At $\gamma \rightarrow 0$, the general expression (22) gives the following low-frequency representation of the average velocity of a ratchet with the extremely asymmetric stationary part $u(x)$ of the nanoparticle potential energy:

$$\begin{aligned} \frac{\langle v \rangle}{v_0} &\xrightarrow{\gamma \rightarrow 0} \frac{\alpha\gamma \varphi_3(\alpha)}{2\varphi_1^2(\alpha)} [2\varphi_3(\alpha) + \cos 4\pi \lambda_0], \\ \varphi_3(\alpha) &= \frac{\alpha^2}{\alpha^2 + 4\pi^2}. \end{aligned} \quad (25)$$

It is easily shown that, at $\gamma \rightarrow 0$, the high-temperature expression (24) gives the result coinciding with the high-temperature limit ($\alpha \rightarrow 0$) of the expression (25), that is,

$$\frac{\langle v \rangle}{v_0} \xrightarrow[\gamma \rightarrow 0]{\alpha \rightarrow 0} \frac{1}{8\pi^2} \alpha^3 \gamma \cos 4\pi \lambda_0, \quad (26)$$

as expected. Relations (24)–(26) lead to a number of important conclusions. In the region of high temperatures ($\alpha \ll 1$), the motion direction is determined by the sign of the function $\cos 4\pi \lambda_0$. For example, for the values of the phase shift within the interval $0 < \lambda_0 < 1/2$, the average velocity is positive at $\lambda_0 < 1/8$ and $\lambda_0 > 3/8$, while it is negative for $1/8 < \lambda_0 < 3/8$ (Fig. 4). At sufficiently low temperatures, $T < T_c^{(\text{low})}$ with

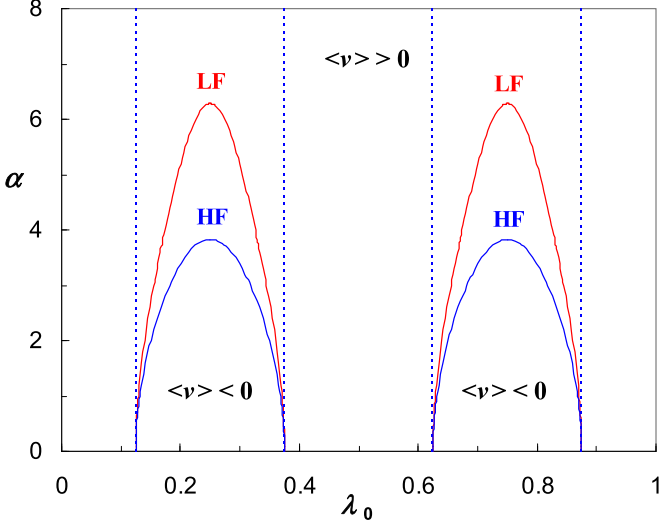


FIG. 4. Phase diagram in the space of parameters α and λ_0 (inverse temperature–phase-shift space), demonstrating the ranges of values within which different directions, leftward (inner regions) and rightward (outer regions), of the ratchet motion can occur. Zero-velocity contours are plotted for low-frequency and high-frequency approximations (LF and HF curves, respectively).

$T_c^{(\text{low})} \approx 0.159 u_0/k_B$ ($\alpha_c^{(\text{low})} = 2\pi$), the velocity sign is always (i.e., for any phase shift λ_0) positive. In Fig. 4, the value $T_c^{(\text{low})}$ determines the α value corresponding to the maxima of low-frequency (LF) curves. Finally, in the region of intermediate temperature values $T > T_c^{(\text{low})}$ and at low frequencies, one can reverse the motion direction by tuning the value of the phase shift λ_0 (Fig. 4); this follows from the competition of the terms in the square brackets in (25).

The high-frequency behavior can be obtained from (22) with $\gamma \rightarrow \infty$:

$$\frac{\langle v \rangle}{v_0} \xrightarrow{\gamma \rightarrow \infty} \frac{2\pi^2 \alpha^2}{\gamma \sinh \alpha} \left[\cos 4\pi \lambda_0 + \frac{\alpha/2}{\tanh \alpha/2} - 1 \right]. \quad (27)$$

Intersection of regions $\alpha \rightarrow 0$ and $\gamma \rightarrow \infty$ in the (α, γ) plane determines the common applicability domain of the expressions (24) and (27), where they are both reduced to the following simple form:

$$\frac{\langle v \rangle}{v_0} \xrightarrow[\gamma \rightarrow \infty]{\alpha \rightarrow 0} \frac{2\pi^2 \alpha}{\gamma} \cos 4\pi \lambda_0. \quad (28)$$

While in the region of high temperatures the motion direction is still determined by the sign of the function $\cos 4\pi \lambda_0$, at $T < T_c^{(\text{high})}$ with $T_c^{(\text{high})} \approx 0.261 u_0/k_B$ [$\alpha_c^{(\text{high})} \approx 3.83$, see (27) for clarity; it is the value corresponding to the maxima of high-frequency (HF) curves in Fig. 4], the velocity remains always positive. Therefore, from this, supplemented with the above result concerning $T_c^{(\text{low})}$, we conclude that for intermediate values of both temperatures $T_c^{(\text{low})} < T < T_c^{(\text{high})}$ ($3.83 < \alpha < 6.28$) and frequencies (the area between LF and HF curves in Fig. 4), controlling the motion direction becomes possible not only through the phase shift λ_0 , but also by tuning the temperature and frequency. Figure 4 is a phase diagram in $\alpha - \lambda_0$ variables; it shows families of stopping points in the

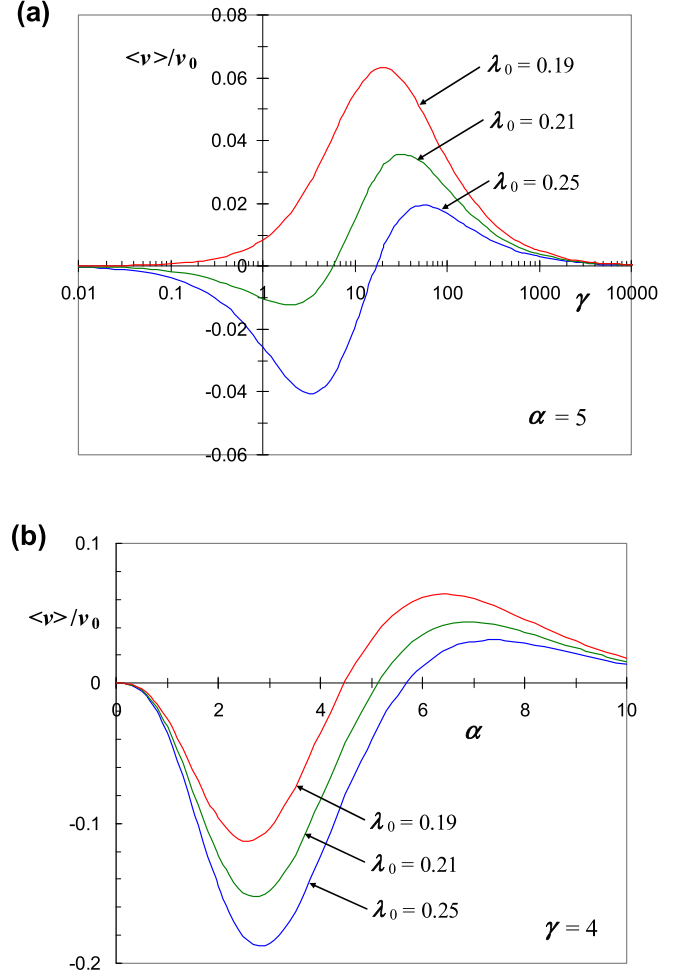


FIG. 5. Analytical dependences of the average motor velocity with an extremely asymmetric ($l = L$) sawtooth potential $u(x)$ on the dimensionless frequency parameter γ at a fixed value of the temperature parameter $\alpha = 5$ (a) and on the temperature parameter α at a fixed γ value $\gamma = 4$ (b).

low- and high-frequency regimes. These contours divide the diagram into regions of positive and negative values of the average velocity. Thus, in the regions above the LF curves and below the HF curves, the direction of the particle flux is fixed, rightward and leftward, respectively, while the inner region between the LF- and HF curves includes those α and λ_0 values, at which one can get either rightward or leftward flux, depending on γ values; this is what makes this inner region interesting.

VI. TEMPERATURE-FREQUENCY CONTROL OF RATCHET OPERATING MODES

In the range of intermediate values of frequencies and temperatures (see Fig. 4 and the corresponding discussions in Sec. V), analytical solution (22) of the extremely asymmetric model demonstrates the possibility of reversing the motion direction by tuning the frequency γ [Fig. 5(a)] or temperature α [Fig. 5(b)]. The analysis of this solution shows that, at certain values of the phase shift λ_0 , changing γ and α yields only one change in the motion direction (i.e., a single stopping

point can exist). We can illustrate the way the stopping point appears under changes in fluctuation frequency γ by fixing the value of the temperature parameter, say, let $\alpha = 5$. Then, the velocity is positive in the high-frequency region at any λ_0 values, while it becomes negative in the low-frequency region if $0.195 < \lambda_0 < 0.304$ (Fig. 4). Therefore, for the λ_0 values belonging to that interval, say, $\lambda_0 = 0.21$ and 0.25 , the stopping point will appear for the intermediate values of the frequency γ , whereas at $\lambda_0 = 0.19$ (which is out of the interval) the velocity remains positive at any frequencies, and the stopping point will never appear [Fig. 5(a)]. Similarly, in the region of low temperatures ($\alpha \gg 1$), the velocity is positive at any λ_0 value, while in the region of high temperatures ($\alpha \ll 1$), it is negative for $1/8 < \lambda_0 < 3/8$ (Fig. 4). Thus, at any frequencies, in that range of λ_0 values, the temperature dependence of the velocity will have one stopping point [Fig. 5(b) is an example here].

The fact that the results just discussed are nontrivial (different from the more predictable nonextremely asymmetric case) becomes clear from the analysis of an extended model in which the potential $u(x)$ is sawtooth but nonextremely asymmetric ($l \neq 0, L$). Let us come to it. The high-frequency asymptotics of the average ratchet velocity calculated from (7) with the sawtooth $u(x)$ without jumps leads to the following expression:

$$\frac{\langle v \rangle}{v_0} \xrightarrow{\gamma \rightarrow \infty} -\frac{\pi \alpha}{\gamma \varphi_1^2(\alpha)} f(l, \lambda_0) \xrightarrow{l \rightarrow L} \frac{2\pi^2 \alpha}{\gamma \varphi_1^2(\alpha)} \cos 4\pi \lambda_0, \quad (29)$$

in which the function $f(l, \lambda_0)$ is defined in (23). We will compare asymptotic behavior of the ‘‘arbitrarily asymmetric result’’ (29) ($l \neq L$) in the limit $l \rightarrow L$ with the behavior of the ‘‘extremely asymmetric result’’ (27) ($l = L$), valid for arbitrary temperatures. The limiting value of the average velocity (29), corresponding to the geometry $l \rightarrow L$, coincides with its value (27) (valid for $l = L$) at high temperatures ($\alpha \rightarrow 0$) though differs at low temperatures ($\alpha \gg 1$). In its turn, the high-frequency asymptotics (29) at $l \rightarrow L$ yields negative values of the average velocity in the intervals $\lambda_0 \in (1/8, 3/8)$ and $(5/8, 7/8)$ for arbitrary temperatures, including low ones; this fact does not imply the occurrence of stopping points with a change in temperature. However, according to the ‘‘extremely asymmetric result’’ (27), the velocity sign can become positive in the above intervals of λ_0 values when the temperatures are sufficiently low ($\alpha \gg 1$). All this means that it is the special form of the high-frequency asymptotic behavior of the average velocity of the ratchet with the extremely asymmetric potential ($l = L$) which is in charge for the appearance of a stopping point at low temperatures. This behavior differs from the high-frequency asymptotic behavior of the ratchet with $L-l$ small but different from zero, $l \neq L$ [compare expressions (27) and (29)]. In Sec. VII, we discuss the physical meaning of this difference between the limiting velocity value at $l \rightarrow L$ and its value at the point $l = L$.

Let us come to the frequency-dependent behavior. To deepen the analysis of the dependence of the velocity sign on the perturbation frequency, we use numerical results obtained for arbitrary sawtooth potentials (of an arbitrary asymmetry l). Such calculations can be performed either by numerical integration of expression (2) with the Green function $S(x, y)$

of the explicit form presented in [24] or by using the Fourier analog of the expression (2):

$$\langle v \rangle = -iL^3 \beta^2 D^2 \sum_{pp'p_1p_2} k_p k_{-p-p_1} k_{-p_2+p'} \rho_{p_1}^{(+)} \rho_{p_2}^{(-)} \times S_{pp'} w_{-p-p_1} w_{-p_2+p'}. \quad (30)$$

Here the quantities $\rho_p^{(\pm)}$, w_p , and $S_{pp'}$ are the Fourier components of the periodic functions $\rho_{\pm}(x)$, $w(x)$, and $S(x, y)$, respectively, and $k_p = 2\pi p/L$ ($p = 0, \pm 1, \pm 2, \dots$) is the wave vector. The quantities $S_{pp'} = L^{-2} \int_0^L dx \int_0^L dy S(x, y) e^{-ik_p x + ik_{p'} y}$, in accordance with (6) [taking into account (5)], can be calculated as matrix elements of the inverse of the matrix specified by its elements $-L[(Dk_p^2 + \Gamma)\delta_{pp'} + \beta Dk_p k_{p-p'} u_{p-p}]$. This was the method which we followed to calculate the frequency dependences in Fig. 6.

We chose the widths of the links of the sawtooth potential such that its shape was close to the extremely asymmetric shape ($l \rightarrow L$). Note that since the velocity reverses upon substitutions $l \rightarrow L-l$ and $\lambda_0 \rightarrow 1/2 - \lambda_0$ [see the symmetry property (B8) in Appendix B], the limiting behavior $l \rightarrow 0$ can be analyzed in a similar way. The frequency dependences in Fig. 6 show that in the low-frequency region, the curves with $l \rightarrow L$ do tend to the curve with $l = L$. However, in the high-frequency region, at certain values of the phase shift λ_0 , the curves with $l \rightarrow L$ tend to the abscissa axis from below, while the curve with $l = L$ tends to the abscissa axis from above. The consequences of this are as follows. If there are no stopping points for the extremely asymmetric potential $u(x)$ with $l = L$, then in case of $u(x)$ infinitesimally close (but different) to it, $l \rightarrow L$, the stopping points arise [curve 2 in Fig. 6(a), and curves 2–4 in Fig. 6(b)]. And vice versa, if there exists a stopping point for the potential with $u(x) l = L$, then at $l \rightarrow L$ this point can disappear [curves 2–4 in Fig. 6(c), curves 3,4 in Fig. 6(d), and curves 2–4 in Fig. 6(e)]. Note that additional stopping points can arise as a result of transition of the ratchet system from the geometry $l = L$ to the geometries $l \rightarrow L$: Two stopping points characterize curve 2 in Figs. 6(a) and 6(d). Why it is so, we will discuss in the next section.

VII. DISCUSSION AND CONCLUSIONS

The performed analysis of the ratchet effect in a sawtooth potential, dichotomously modulated by a spatially harmonic perturbation, led us to several groups of results. The first group includes the explicit expression for the Laplace image of the Green function of the extremely asymmetric sawtooth potential and using this expression (within the approximation of slightly fluctuating potential energy) for analytically integrating the relations for the average velocity of a Brownian particle. The results of the second group concern the analysis of the frequency and temperature dependences of the obtained expression for the average velocity. They also include the comparison of its high-temperature, low-frequency, and high-frequency asymptotics with the analogous asymptotics for the ratchet with a sawtooth potential of arbitrary (not extreme) asymmetry. The third group is the results of numerical calculations and the deriving the ratchet symmetry properties

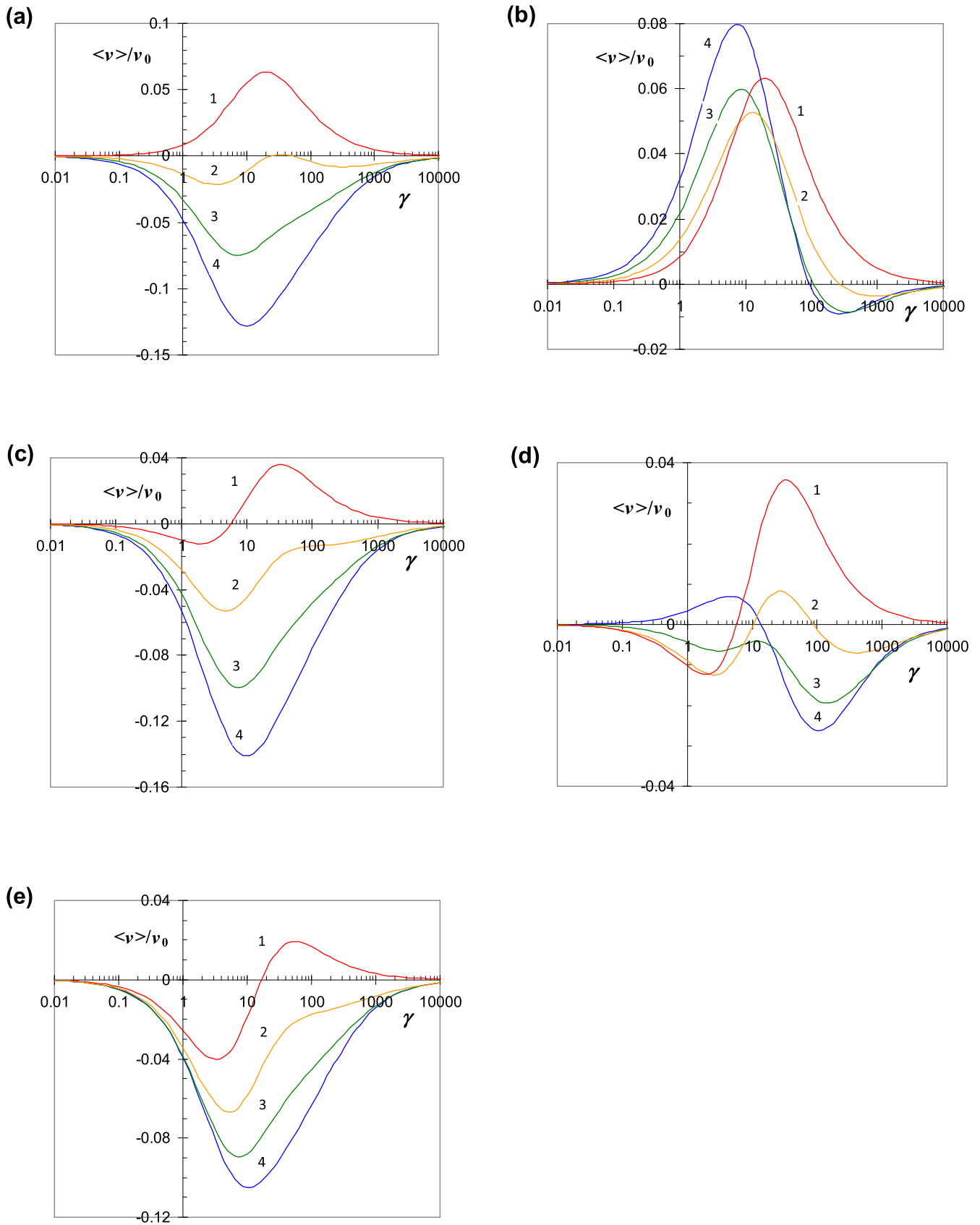


FIG. 6. Frequency dependences of the average velocity at the inverse temperature value $\alpha = 5$ calculated for various values of the phase shift: $\lambda_0 = 0.19$ (a), 0.31 (b), 0.21 (c), 0.29 (d), and 0.25 (e). The curve numbers correspond to different asymmetries of the sawtooth profile $u(x)$: $l/L = 1$ (1), 0.975 (2), 0.95 (3), and 0.925 (4).

with neither applying the approximations of the overdamped regime and small fluctuations nor the choice of a dichotomous process to control fluctuations.

The main conclusion from all the results obtained concerns the possibility of frequency-temperature controlling the magnitude and direction of the ratchet velocity. Known solution of a similar problem within the high-temperature approximation indicated that changing the motion direction could be only through tuning the phase shift of the spatial harmonic disturbance relative to the stationary sawtooth component [34]. Within that approximation, the frequency dependence of the average velocity was a simple constant-sign bell-shaped function. The analytical solution obtained in this paper shows that only at sufficiently low temperatures and in certain intervals of the phase-shift values the frequency dependence becomes sign alternating; this fact determines the frequency-controlled reversal of the motion direction. Conversely, at certain frequencies and phase shifts, it becomes possible to reverse the motion direction by a change in temperature.

Another nontrivial feature of the analytical expression for the ratchet velocity, obtained here for the case of the extremely asymmetric sawtooth $u(x)$, is that the high-frequency velocities of this ratchet and of the same ratchet but with the sawtooth $u(x)$ of arbitrary (not extreme) asymmetry are opposite in sign to each other. This is due to the fact that the sawtooth potential is characterized by the particle sliding time $\tau_{L-l} = \zeta(L-l)^2/u_0$ along its segment $L-l$, and this time tends to zero with $l \rightarrow L$ in the extremely asymmetric geometry (with the jumplike potential segment $L-l$), thus becoming a new characteristic time of the system. Hence, the high-frequency asymptotic behavior depends on the order of the limits, over the frequency and the inverse sliding time; the obtained sign difference is caused by the competition of these quantities. Such a dependence of the result on the order of limits leading to different high-frequency asymptotics of the average velocity was known before within the high-temperature approximation [29]. Note that nontrivial effects can also be caused by the competition of the tending to zero parameter τ_{L-l} with other times, e.g., the durations of fast perturbing processes of the relaxation type [25,31] or the characteristic time associated with the finite particle mass [30].

Next, let us discuss the physical meaning of the dependence of the average velocity on the order of limits $l \rightarrow L$ and $\Gamma \rightarrow \infty$ as well as reveal the mechanism of how an additional stopping point can originate from this dependence. The above analyzed “extremely asymmetric ratchet” ($l = L$) could have only one stopping point in frequency dependences of the velocity. Let us deepen the nonextremely asymmetric case ($l \neq L$). At large values of τ_{L-l}^{-1} and Γ , the question of fundamental importance is which of the inequalities, either $\Gamma < \tau_{L-l}^{-1}$ or $\Gamma > \tau_{L-l}^{-1}$, is fulfilled. In the first case, $\Gamma < \tau_{L-l}^{-1}$, one can simply set $l = L$ and $\tau_{L-l} = 0$ (the case $l = L$); then the inequality $\Gamma < \tau_{L-l}^{-1}$ is considered to be satisfied for any Γ values. This case corresponds to curve 1 in Fig. 6(d), with only one stopping point; it is the case we have been discussing. This stopping point occurs because the average velocity is negative at low Γ while it is positive at high Γ . Therefore, with a change in the frequency parameter γ from zero to infinity,

the continuous frequency dependence of the average velocity certainly crosses the abscissa axis.

In the second case $l < L$ and $\tau_{L-l} > 0$, so there will exist a region (absent in the first case) in which the frequency is so high that it is even higher than τ_{L-l}^{-1} , $\Gamma > \tau_{L-l}^{-1}$. Then, at $\Gamma \rightarrow \infty$, when one tunes the fluctuation frequency to this new region, the sign of the high-frequency asymptotics of the average velocity is opposite to its sign in the first case [see the discussion concerning Eqs. (27) and (29) in Sec. V]. On the other hand, since the values τ_{L-l}^{-1} and Γ remain large, in the region $\Gamma < \tau_{L-l}^{-1}$, the velocity sign will be the same as the sign of the high-frequency asymptotics of the first ($\tau_{L-l} = 0$) case. All this means that, in the region $\Gamma > \tau_{L-l}^{-1}$, a second stopping point appears, additional to the point observed for frequencies $\Gamma < \tau_{L-l}^{-1}$ [see curve 2 in Fig. 6(d)].

In conclusion, we emphasize that the results presented in this paper illustrate the rare case when rather abstract results (about the dependence of the system behavior on the order of limits) can lead to those of practical importance. Indeed, an extremely asymmetric sawtooth potential is hardly realizable experimentally, so it would seem that knowing the high-frequency asymptotics of the ratchet velocity in such a potential is of little use. Nevertheless, this information turns out to be of fundamental importance, since it explains how one can get a second stopping point in the high-frequency region for real, not extremely asymmetric, potentials. Here, it will be useful to note that one of the main mechanisms of motion reversal in ratchet systems is the competition between the spatial and temporal asymmetry of the potential energy [35]. For flashing and rocking ratchets, the average velocity depends on parameters of spatial and temporal asymmetry in different fashion, namely, multiplicatively and additively, respectively [35,36]. This makes motion reversal most easily achieved for rocking ratchets [37] than for flashing ones provided the same shapes of the functions $u(x)$ and $w(x)$ in Eq. (1) [35,36]. The approximation of small fluctuations, in which the ratchet effect is proportional to the second degree of the perturbation $w(x)$, excludes taking the temporal asymmetry into account. On the other hand, when the profiles $u(x)$ and $w(x)$ are different and there is a shift λ_0 between their symmetry axes, it becomes possible to regulate the motion direction not only by changing λ_0 , but also by using the fact of competition of other time parameters, e.g., the sliding time and the correlation time of the dichotomous noise. Thus, summarizing what has been said, one can assert that the exactly solvable model of a slightly fluctuating pulsating (flashing) ratchet developed in this paper, combined with both the symmetry analysis and numerical results of a more general model, has convincingly demonstrated that, in specific systems, highly nontrivial mechanisms can underlie the possibility of frequency-temperature controlling the intensity and direction of the ratchet effect.

ACKNOWLEDGMENTS

This work was carried out within the framework of the State Assignment No. 45.22 (Registration No. AAAA-A18-118012390045-2) and supported by the Russian Foundation for Basic Research (Projects No. 20-57-00007_Bel_a and No.

21-57-52006_MNT_a) and the Belarusian Republican Foundation for Basic Research (Project No. F20R-032).

APPENDIX A: PERTURBATION THEORY IN SMALL FLUCTUATIONS

Let us write the Smoluchowski equation in the form of the continuity equation

$$\frac{\partial}{\partial t}\rho(x, t) + \frac{\partial}{\partial x}J(x, t) = 0, \quad (\text{A1})$$

with the probability flux $J(x, t)$ determining by

$$J(x, t) = \hat{J}(x)\rho(x, t) - \beta D w'(x)\sigma(t)\rho(x, t). \quad (\text{A2})$$

Using the retarded Green function $g(x, y, t)$ of diffusion in the stationary potential relief $u(x)$, which satisfies Eq. (4), one can equivalently represent Eq. (A1) as the following integral equation:

$$\rho(x, t) = \rho_-(x) - \beta D \int_0^L dy \int_{-\infty}^{\infty} dt' g(x, y, t - t') \sigma(t') \times \frac{\partial}{\partial y} [w'(y)\rho(y, t')]. \quad (\text{A3})$$

Here the unperturbed distribution function $\rho_-(x)$ satisfies the equation $\hat{J}(x)\rho_-(x) = 0$, which is the condition for the unperturbed flux to vanish. The normalized solution of this equation is the Boltzmann distribution $\rho_-(x) = e^{-\beta u(x)} / \int_0^L dx e^{-\beta u(x)}$. The validity of the representation (A3) can be verified by time differentiating both its sides; this, when using Eq. (4), brings Eq. (A3) back to the original Smoluchowski equation of the form (A1) with (A2).

Next, we multiply (term by term) the equation for the probability flux (A2) by $\exp[\beta u(x)]$ and integrate the result over the spatial period L . Since the integral of the derivative of a periodic function over its period is zero, we obtain the following identity:

$$\int_0^L dx e^{\beta u(x)} J(x, t) = -\beta D \int_0^L dx e^{\beta u(x)} w'(x) \sigma(t) \rho(x, t). \quad (\text{A4})$$

Let the operation of averaging over fluctuations $\sigma(t)$ be denoted as $\langle \dots \rangle$. Applying this operation to the continuity equation (A1), we conclude that while $\langle \rho(x, t) \rangle$ depends only on the coordinate, the average flux value $\langle J(x, t) \rangle$ depends neither on time nor on the coordinate, that is, it is a constant. This constant value, multiplied by the spatial period L of the potential energy $u(x)$, determines the average motion velocity $\langle v \rangle = L \langle J(x, t) \rangle$, which is the main characteristic of a Brownian motor. Let us now apply the averaging operation to Eq. (A4). The left-hand side of this equation takes the form $\langle J(x, t) \rangle \int_0^L dx e^{\beta u(x)}$, so that

$$\langle v \rangle = -L\beta D \int_0^L dx \rho_+(x) w'(x) \langle \sigma(t) \rho(x, t) \rangle, \quad (\text{A5})$$

where $\rho_+(x) = e^{\beta u(x)} / \int_0^L dx e^{\beta u(x)}$. Substituting (A3) into (A5) and taking into account the equality $\langle \sigma(t) \rangle = 0$, we get

$$\langle v \rangle = L(\beta D)^2 \int_0^L dx q(x) w'(x) \int_0^L dy \int_{-\infty}^{\infty} dt' g(x, y, t - t') \times \frac{\partial}{\partial y} [w'(y) \langle \sigma(t) \sigma(t') \rho(x, t) \rangle]. \quad (\text{A6})$$

Next, we assume that the function $w(x)$ is small. Then, accurate up to the terms which are quadratic in $w(x)$, we can assume that $\langle \sigma(t) \sigma(t') \rho(x, t) \rangle \approx \langle \sigma(t) \sigma(t') \rangle \rho_-(x)$ [see Eq. (A3)]. Introduce the correlation function $K(t-t') \equiv \langle \sigma(t) \sigma(t') \rangle$ and the function $S(x, y)$ determined by Eq. (3); this makes it possible to pass to the relation (2), which is the main result of the approximation of small fluctuations [25]. Note that this relation has a general character. Firstly, it is valid not only for flashing ratchets discussed in this paper, but also for rocking ratchets. Secondly, it is valid not only for the stochastic dichotomous process considered here in which the correlation function has the form $K(t) = \exp(-\Gamma|t|)$, but also for periodic processes, for which $\sigma(t + \tau) = \sigma(t) = \sum_j \sigma_j \exp(-i\omega_j t)$, where τ is the period, $\omega_j = 2\pi j/\tau$, $j = 0, \pm 1, \pm 2, \dots$, and σ_j is the Fourier component of the function $\sigma(t)$. For such processes, the averaging operation $\langle \dots \rangle$ means averaging over the period, so that $\langle \sigma(t) \rangle = \sigma_0 = 0$, and the correlation function will be written in the form $K(t) = \sum_j |\sigma_j|^2 \exp(-i\omega_j t)$.

Note that the perturbation theory is a powerful apparatus of modern theoretical physics [38,39] and is widely used to describe ratchet systems (see review in Ref. [24] and the literature therein). If the Green function (the resolvent) of an unperturbed system is known, then the characteristics of the perturbed system can be determined using iterations of the Dyson equation [40] [similar to how the result (2) is obtained from Eq. (A3)]. A similar quantum-mechanical perturbation theory has been used for weakly driven quantum coherent ratchets in cold-atom systems [41]. Various versions of the perturbation theory turn out to be useful when considering more complex ratchet systems with feedback, for which it is difficult to obtain analytical solutions [42]. One can expect that the perturbation theory can also be applied for calculating the second moment of the distribution function, the dispersion, and the Péclet number. This would make it possible not only to obtain the average velocity of particle directed motion, but also to characterize synchronization regimes, the coherence, and reproducibility of the ratchet effect [43,44].

APPENDIX B: SYMMETRY PROPERTIES

Let us analyze symmetry properties of a ratchet with a saw-tooth potential of the symmetry described by the parameter l ; the spatial dependence of fluctuations is given by the first harmonic with the phase shift λ_0 (Fig. 3). We will characterize the space-time dependence of the potential energy, of the additive-multiplicative form (1), by the indices l and λ_0 ,

$$U_{l,\lambda_0}(x, t) = u_l(x) + \sigma(t) w_{\lambda_0}(x). \quad (\text{B1})$$

We also assume that the function $u_l(x)$ belongs to the class of antisymmetric functions, while the functions $w_{\lambda_0}(x)$ and $\sigma(t)$ are of the universal symmetry type. According to the

terminology introduced in Ref. [36], a periodic function $f(x)$ (L is its period) belongs to the symmetric, antisymmetric, and shift-symmetric functions under the following properties:

$$\begin{aligned} f_s(x + x_s) &= f_s(-x + x_s), & f_a(x + x_a) &= -f_a(-x + x_a), \\ f_{sh}(x + L/2) &= -f_{sh}(x), \end{aligned} \quad (\text{B2})$$

respectively (x_s is the position of a symmetry axis, x_a is the position of a center of symmetry); the universal symmetry is realized when all three conditions (B2) are simultaneously satisfied. When written for potential energies, transformations (B2) also allow shifts along the ordinate axis, since potential energies are determined up to an arbitrary constant. The time dependence $\sigma(t)$ of the universal symmetry type corresponds to a symmetric dichotomous process with equal average durations of its two states [36]. The average velocity of a ratchet driven by fluctuations of the periodic potential energy of a nanoparticle (flashing ratchet) is a functional of the potential energy with the following symmetry properties [36]:

$$v\{U(x, t)\} \underset{(\text{vect})}{=} -v\{U(-x, t)\}, \quad (\text{B3})$$

$$v\{U(x + x_0, t + t_0)\} \underset{(\text{shift})}{=} v\{U(x, t)\},$$

$$v\{U(x, t)\} \underset{(\text{C-R})}{=} v\{-U(-x, -t)\}. \quad (\text{B4})$$

Relations (B3) describe vector and shift symmetries, which are of a general nature; relation (B4) reflects the hidden Cubero-Renzoni symmetry [45], inherent only in the overdamped regime.

The choice of the origin as it is shown in Fig. 3 accompanied by the replacement $x \rightarrow -x$ leads to the following obvious identities:

$$\begin{aligned} u_l(-x) &= u_{L-l}(x), & w_{\lambda_0}(-x) &= w_{1-\lambda_0}(x), \\ U_{l,\lambda_0}(-x, t) &= U_{L-l,1-\lambda_0}(x, t). \end{aligned} \quad (\text{B5})$$

They make it possible to prove a number of important symmetry properties of the ratchet model under consideration.

First, let us prove that the substitutions $l \rightarrow L-l$ and $\lambda_0 \rightarrow 1 - \lambda_0$ lead to the reversal of the motion direction. This property follows from the chain of transformations:

$$v\{U_{l,\lambda_0}(x, t)\} \underset{(\text{vect})}{=} -v\{U_{l,\lambda_0}(-x, t)\} = -v\{U_{L-l,1-\lambda_0}(x, t)\}. \quad (\text{B6})$$

The second property uses the identity $w_{\lambda_0-1/2}(x) = -w_{\lambda_0}(x)$, which follows from (i) the explicit form of the function $w_{\lambda_0}(x)$ given by the formula (21), according to which $w_{\lambda_0}(x + L/2) = w_{\lambda_0-1/2}(x)$, and (ii) the fact that $w_{\lambda_0}(x)$ is a shift-symmetric function [$w_{\lambda_0}(x + L/2) = -w_{\lambda_0}(x)$]. Then the following chain of equalities holds:

$$\begin{aligned} v\{U_{l,\lambda_0-1/2}(x, t)\} &= v\{u_l(x) - \sigma(t)w_{\lambda_0}(x)\} \\ &\underset{(\text{shift})}{=} v\{u_l(x) - \sigma(t + \tau/2)w_{\lambda_0}(x)\} \\ &= v\{u_l(x) + \sigma(t)w_{\lambda_0}(x)\} = v\{U_{l,\lambda_0}(x, t)\}, \end{aligned} \quad (\text{B7})$$

in which the shift symmetry of the function $\sigma(t)$ with the period τ is used, $\sigma(t + \tau/2) = -\sigma(t)$. Combining equalities (B6) and (B7) gives $v\{U_{l,\lambda_0-1/2}(x, t)\} = -v\{U_{L-l,1-\lambda_0}(x, t)\}$; and taking into account the replacement $\lambda_0 \rightarrow \lambda_0 + 1/2$, we finally get

$$v\{U_{l,\lambda_0}(x, t)\} = -v\{U_{L-l,1/2-\lambda_0}(x, t)\}. \quad (\text{B8})$$

Note that the function $f(l, \lambda_0)$ that determines, in the overdamped mode, both the high-temperature dependence (23) and high-frequency dependence (29) of the ratchet average velocity on l and λ_0 has the same property $f(l, \lambda_0) = -f(L-l, 1/2 - \lambda_0)$. In contrast to the results of these two approximations, as well as to the approximation of slight fluctuations, used in this paper, the property (B8) is proved for the general case: it remains valid both when the inertia of a Brownian particle is taken into account and for the shift-symmetric time dependence of fluctuations. From the property (B8), in particular, it follows that it is sufficient to analyze the domain $\lambda_0 \in [0, 1/2]$.

An additional symmetry property exists for an extremely symmetric sawtooth potential, for which, when choosing the origin as in Fig. 3, the identity $u_L(-x) = -u_L(x)$ holds. From the explicit form of the function $w_{\lambda_0}(x)$, (21), the equality $w_{\lambda_0}(-x) = -w_{1/2-\lambda_0}(x)$ follows. Using these two equalities, as well as the symmetry of the function $\sigma(t)$, gives

$$\begin{aligned} v\{U_{L,1/2-\lambda_0}(x, t)\} &= v\{u_L(x) - \sigma(t)w_{\lambda_0}(-x)\} \underset{(\text{C-R})}{=} v\{-u_L(-x) + \sigma(-t)w_{\lambda_0}(x)\} \underset{(\text{shift})}{=} \\ &\underset{(\text{shift})}{=} v\{-u_L(-x) + \sigma(-t + t_s)w_{\lambda_0}(x)\} = v\{-u_L(-x) + \sigma(t + t_s)w_{\lambda_0}(x)\} \underset{(\text{shift})}{=} \\ &\underset{(\text{shift})}{=} v\{-u_L(-x) + \sigma(t)w_{\lambda_0}(x)\} = v\{u_L(x) + \sigma(t)w_{\lambda_0}(x)\} = v\{U_{L,\lambda_0}(x, t)\}. \end{aligned} \quad (\text{B9})$$

We stress here that in contrast to the general property (B8), which can also be used when taking inertial effects into account, the obtained symmetry property

$$v\{U_{L,\lambda_0}(x, t)\} = v\{U_{L,1/2-\lambda_0}(x, t)\} \quad (\text{B10})$$

is valid only in the overdamped regime, since it uses the time-reversal operation and the Cubero-Renzoni symmetry [45]. Naturally, this hidden symmetry is an attribute of the solution (22) obtained in the overdamped regime: the entire dependence on λ_0 enters (22) only through the factor $\cos 4\pi\lambda_0$ which is invariant under the replacement $\lambda_0 \rightarrow 1/2 - \lambda_0$.

Note that at $l = L/2$, the antisymmetric sawtooth potential also acquires shift-symmetric properties, $u_{L/2}(x + L/2) = -u_{L/2}(x)$, that is, it becomes a function of the universal symmetry, just like the functions $w_{\lambda_0}(x)$ and $\sigma(t)$ are. This means that there is the property $U_{L/2,\lambda_0}(x, t + t_s) = -U_{L/2,\lambda_0}(x + L/2, -t + t_s)$, which, in the terminology of Refs. [1,46], is an attribute of

the so-called supersymmetric function, for which the ratchet effect is absent,

$$\begin{aligned} v\{U_{L/2,\lambda_0}(x,t)\}_{(\text{shift})} &= v\{U_{L/2,\lambda_0}(x+L/2,t+t_s)\} = v\{-U_{L/2,\lambda_0}(x,-t+t_s)\}_{(\text{shift})} \\ &= v\{-U_{L/2,\lambda_0}(x,-t)\}_{(\text{shift})} = v\{U_{L/2,\lambda_0}(-x,t)\}_{(\text{vect})} = -v\{U_{L/2,\lambda_0}(x,t)\}. \end{aligned} \quad (\text{B11})$$

Here, the use of the Cubero-Renzoni symmetry also means that this property is valid only in the overdamped mode, i.e., in the specified geometry of the system,

a nonzero ratchet velocity can arise when the particle mass changes and thus takes the system out of this regime.

-
- [1] P. Reimann, *Phys. Rep.* **361**, 57 (2002).
- [2] P. Hänggi and F. Marchesoni, *Rev. Mod. Phys.* **81**, 387 (2009).
- [3] S. Denisov, S. Flach, and P. Hänggi, *Phys. Rep.* **538**, 77 (2014).
- [4] D. Cubero and F. Renzoni, *Brownian Ratchets: From Statistical Physics to Bio and Nano-motors* (Cambridge University Press, Cambridge, 2016).
- [5] Yu. V. Gulyaev, A. S. Bugaev, V. M. Rozenbaum, and L. I. Trakhtenberg, *Phys. Usp.* **63**, 311 (2020).
- [6] P. M. Hoffmann, *Rep. Prog. Phys.* **79**, 032601 (2016).
- [7] M. R. Cheetham, J. P. Bramble, D. G. G. McMillan, R. J. Bushby, P. D. Olmsted, L. J. C. Jeuken, and S. D. Evans, *Soft Matter* **8**, 5459 (2012).
- [8] A. Krogh, B. Larsson, G. von Heijne, and E. Sonnhammer, *J. Mol. Biol.* **305**, 567 (2001).
- [9] J. P. Overington, B. Al-Lazikani, and A. L. Hopkins, *Nat. Rev. Drug Discov.* **5**, 993 (2006).
- [10] S. Erbas-Cakmak, D. A. Leigh, C. T. McTernan, and A. L. Nussbaumer, *Chem. Rev.* **115**, 10081 (2015).
- [11] G. Tsiavaliaris, S. Fujita-Becker, and D. J. Manstein, *Nature (London)* **427**, 558 (2004).
- [12] M. Nakamura, L. Chen, S. C. Howes, T. D. Schindler, E. Nogales, and Z. Bryant, *Nat. Nanotechnol.* **9**, 693 (2014).
- [13] J. Bath, S. J. Green, and A. J. Turberfield, *Angew. Chem. Int. Ed.* **44**, 4358 (2005).
- [14] P. Yin, H. M. T. Choi, C. R. Calvert, and N. A. Pierce, *Nature (London)* **451**, 318 (2008).
- [15] T. Omabegho, R. Sha, and N. C. Seeman, *Science* **324**, 67 (2009).
- [16] Y. He and D. R. Liu, *Nat. Nanotechnol.* **5**, 778 (2010).
- [17] K. Lund, A. J. Manzo, N. Dabby *et al.*, *Nature (London)* **465**, 206 (2010).
- [18] S. F. J. Wickham, M. Endo, Y. Katsuda *et al.*, *Nat. Nanotechnol.* **6**, 166 (2011).
- [19] T. G. Cha, J. Pan, H. Chen *et al.*, *Nat. Nanotechnol.* **9**, 39 (2013).
- [20] N. Koumura, R. W. J. Zijlstra, R. A. van Delden, N. Harada, and B. L. Feringa, *Nature (London)* **401**, 152 (1999).
- [21] J. Berna, D. A. Leigh, M. Lubomska, S. M. Mendoza, E. M. Perez, P. Rudolf, G. Teobaldi, and F. Zerbetto, *Nat. Mater.* **4**, 704 (2005).
- [22] V. Serreli, C. F. Lee, E. R. Kay, and D. A. Leigh, *Nature (London)* **445**, 523 (2007).
- [23] B. Lau, J. Kedem, D. Schwabacher *et al.*, *Mater. Horiz.* **4**, 310 (2017).
- [24] V. M. Rozenbaum, I. V. Shapochkina, and L. I. Trakhtenberg, *Phys.-Usp.* **62**, 496 (2019).
- [25] V. M. Rozenbaum, I. V. Shapochkina, S. H. Lin, and L. I. Trakhtenberg, *JETP Lett.* **105**, 542 (2017).
- [26] R. D. Astumian and M. Bier, *Phys. Rev. Lett.* **72**, 1766 (1994).
- [27] A. Mielke, *Ann. Phys. (Leipzig)* **507**, 721 (1995).
- [28] M. L. Dekhtyar, A. A. Ishchenko, and V. M. Rozenbaum, *J. Phys. Chem. B* **110**, 20111 (2006).
- [29] V. M. Rozenbaum, I. V. Shapochkina, S.-Y. Sheu, D.-Y. Yang, and S. H. Lin, *Phys. Rev. E* **94**, 052140 (2016).
- [30] V. M. Rozenbaum, Yu. A. Makhnovskii, I. V. Shapochkina, S.-Y. Sheu, D.-Y. Yang, and S. H. Lin, *Phys. Rev. E* **92**, 062132 (2015).
- [31] I. V. Shapochkina, V. M. Rozenbaum, S.-Y. Sheu, D.-Y. Yang, S. H. Lin, and L. I. Trakhtenberg, *Physica A* **514**, 71 (2019).
- [32] R. D. Astumian, *Science* **276**, 917 (1997).
- [33] J. S. Roth, Y. Zhang, P. Bao, M. R. Cheetham, X. Han, and S. D. Evans, *Appl. Phys. Lett.* **106**, 183703 (1915).
- [34] V. M. Rozenbaum, I. V. Shapochkina, Y. Teranishi, and L. I. Trakhtenberg, *Phys. Rev. E* **99**, 012103 (2019).
- [35] V. M. Rozenbaum, T. Ye. Korochkova, A. A. Chernova, and M. L. Dekhtyar, *Phys. Rev. E* **83**, 051120 (2011).
- [36] V. M. Rozenbaum, I. V. Shapochkina, Y. Teranishi, and L. I. Trakhtenberg, *Phys. Rev. E* **100**, 022115 (2019).
- [37] J. Kula, T. Czernik, and J. Łuczka, *Phys. Rev. Lett.* **80**, 1377 (1998).
- [38] E. M. Lifshitz and L. P. Pitaevskii, *Statistical Physics Pt. 2 Theory of the Condensed State* (Pergamon Press, Oxford, 1980).
- [39] H. Risken, *The Fokker-Plank Equation Methods of Solution and Applications* (Springer-Verlag, Berlin, 1989).
- [40] F. J. Dyson, *Phys. Rev.* **75**, 486 (1949).
- [41] M. Heimsoth, C. E. Creffield, and F. Sols, *Phys. Rev. A* **82**, 023607 (2010).
- [42] T. D. Frank, *Phys. Rev. E* **71**, 031106 (2005).
- [43] P. Romanczuk, F. Müller, and L. Schimansky-Geier, *Phys. Rev. E* **81**, 061120 (2010).
- [44] J. Jarillo, J. P. G. Villaluenga, and F. J. Cao, *Phys. Rev. E* **98**, 032101 (2018).
- [45] D. Cubero and F. Renzoni, *Phys. Rev. Lett.* **116**, 010602 (2016).
- [46] P. Reimann, *Phys. Rev. Lett.* **86**, 4992 (2001).